Mass Spectrometry and Photoelectron Spectroscopy of Tetracene Cluster Anions, (Tetracene)$_n^-$ ($n = 1−100$): Evidence for the Highly Localized Nature of Polarization in a Cluster Analogue of Oligoacene Crystals

Masaaki Mitsui,[†] Naoto Ando,[†] and Atsushi Nakajima*[,†,‡]

Department of Chemistry, Faculty of Science and Technology, Keio University, 3-14-1 Hiyoshi, Kohoku-ku, Yokohama 223-8522, Japan, and CREST, Japan Science Technology Agency, c/o Department of Chemistry, Keio University, Yokohama, 223-8522, Japan

Photoelectron spectroscopy of tetracene cluster anions, (tetracene)$_n^-$ ($n = 1−100$), reveals the coexistence of two types of isomers, designated as isomers I and II-1 ($n = 10−50$) or isomers I and II-2 ($n > 60$), in a wide size range. The vertical detachment energies (VDEs) of isomer I increase persistently due to polarization and structural relaxation effects, where a monomeric anion core is encompassed with geometrically reorganized neutral molecules. Conversely, a characteristic ion distribution in the mass spectrum of (tetracene)$_n^-$ ensues from the two-dimensional (2D) herringbone-type ordering of isomer II-1, whose VDEs remain constant at 1.80 eV for $n \geq 14$. Also, isomer II-2, presumably adopting multilayered structural motifs, exhibits invariable VDEs of 2.0 eV, a manifestation of significant charge screening effects in these isomers. The invariable nature of the VDEs of isomers II-1 and II-2 unambiguously demonstrates a largely localized nature of polarization induced by the excess charge residing in microscopic crystal-like environments. Surprisingly, only 14 tetracene molecules within a 2D herringbone-type layer including an excess charge can provide the charge stabilization energy corresponding to ∼80% of that of the crystal, and the rest of the energy is provided by polarization of neutral molecules in adjacent layers.

A unique characteristic of organic molecular crystals (OMCs) is that, because they interact by weak intermolecular van der Waals interactions, the molecules preserve their molecular identity to a large extent. This feature results in narrow electronic bandwidths, and electron/hole charge carriers in OMCs are often strongly localized on individual molecules, that is, molecular ions are formed. Such a molecular ion is instantaneously stabilized by the electronic polarization of its neutral neighbors, which significantly affects the positions of charge-transport energy levels, that is, the highest-occupied molecular orbital (HOMO) and the lowest-unoccupied molecular orbital (LUMO), in OMCs.[1,2]

Because a single molecular ion is stabilized by the finite number of surrounding neutral molecules, organic molecular cluster ions are expected to offer a new avenue to afford a better microscopic description of the charge localization phenomena in OMCs. In particular, photoelectron (PE) spectroscopy of the molecular cluster anions can provide direct information on the energy of the LUMO, electron-vibrational coupling, and, in some cases, charge delocalization (or charge resonance) effects at a specific size and geometry. Since the mass selection of cluster anions can be readily performed in the PE spectroscopy measurements, energetics of the LUMO from an isolated

molecule to the bulk can be exactly traced as a function of cluster size, n.

Among the class of OMCs, linear oligoacenes such as tetracene and pentacene are representative examples for the study of charge-carrier localization and transport.[1−7] Furthermore, recent interest in their fundamental properties has undergone a renewal because of their promising potential for organic electronics applications.[2−5] However, few efforts have been hitherto invested in the study of oligoacene cluster anions,[8−12] especially in the large size region.[11,12] Here, we present the first report of mass spectrometry and PE spectroscopy of tetracene cluster anions, (tetracene)$_n^-$ ($n = 1−100$), and discuss the size evolution of their electronic and geometric structures.

Tetracene vapors in He carrier gas at 10−70 atm pressure are expanded into vacuum using a Even−Lavie valve[13] heated to 300 °C. Cluster anions produced by the electron impact ionization method continue through a skimmer to a linear time-of-flight spectrometer, where a pulsed electric field directs the cluster anions toward a magnetic bottle photoelectron spectrometer.[14] When the target anions reach the magnetic bottle, they are photodetached with 1064 (1.165 eV), 532 (2.331 eV), or 355 nm (3.496 eV) photons from a Nd:YAG laser. The energy resolution is about 50 meV for 1 eV photodetached electrons.

Figure 1 displays mass spectra of (tetracene)$_n^-$ measured for (a) an early part and (b) a late part of the anion beam expanding from the valve at a stagnation pressure of 70 atm. In Figure 1a,

* To whom correspondence should be addressed. Fax: +81-45-566-1697. E-mail: nakajima@chem.keio.ac.jp.
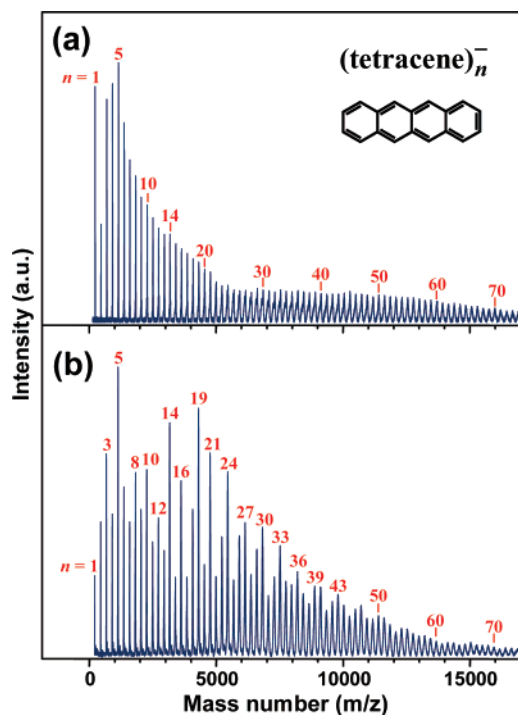† Faculty of Science and Technology, Keio University.
‡ CREST.

Letters

J. Phys. Chem. A, Vol. 111, No. 39, 2007 **9645**

Figure 1. Mass spectra of tetracene cluster anions, $(tetracene)_n^-$, recorded for (a) an early part and (b) a late part of the anion beam expanding from the valve at a stagnation pressure of 70 atm.

a smooth mass distribution is observed, while Figure 1b exhibits some striking features, including the even−odd alternation ($3 < n < 14$), the strong magic numbers of $n = 5$, 14, and 19, and the periodical intensity oscillation of $\Delta n = +2$ or $+3$ (e.g., $n = 14$, 16, 19, 21, 24, 27, and 30). These local maxima observed here are clearly different from those predicted on the basis of LJ interactions between hard spheres,[15] for example, $n = 13$, 19, 23, 26, 29, and 32. Considering an anisotropic "rodlike" molecular structure of tetracene, a plausible structural motif for its relatively small clusters is one with two-dimensional (2D) ordering, where all tetracene molecules interact with their long molecular axes in parallel. Indeed, the tetracene single crystals formed by the physical vapor transport prefer to grow in the direction to maximize π-orbital overlap (or $\pi-\pi$ interaction) between adjacent molecules (i.e., parallel to the herringbone plane).[4]

The $n = 14$ cluster is the most "persistent" magic number that frequently appears under various cluster formation conditions. Hence, it presumably must possess a geometrically closed structure. As illustrated in Figure 2a, we propose that the $n = 14$ cluster adopts a 2D herringbone-type ordering, which is a finite-size analogue of the 2D herringbone layer found in the tetracene crystal. In this structure, all of the long molecular axes are parallel, and the central four molecules are completely surrounded by 10 other molecules; namely, this 14-mer unit constitutes the first 2D shell closing for the tetramer core. For the size range of $n = 15-30$, we also propose that additional molecules, labeled 15−30, two-dimensionally enclose the 14-mer unit in a stepwise fashion, filling the second 2D shell for the tetramer core, as shown in Figure 2b.

Appealingly, this picture perfectly explains the characteristic mass distribution of $n \geq 14$ as follows. When the second 2D shell is partly filled and this yields a more or less geometrically closed structure, it is called a subshell closing.[16] In Figure 2b, such a condition is encountered at the numbers of 16, 19, 21, 24, 27, and 30, where all of the molecules of the second 2D shell interact with three or four neighboring molecules. Indeed,
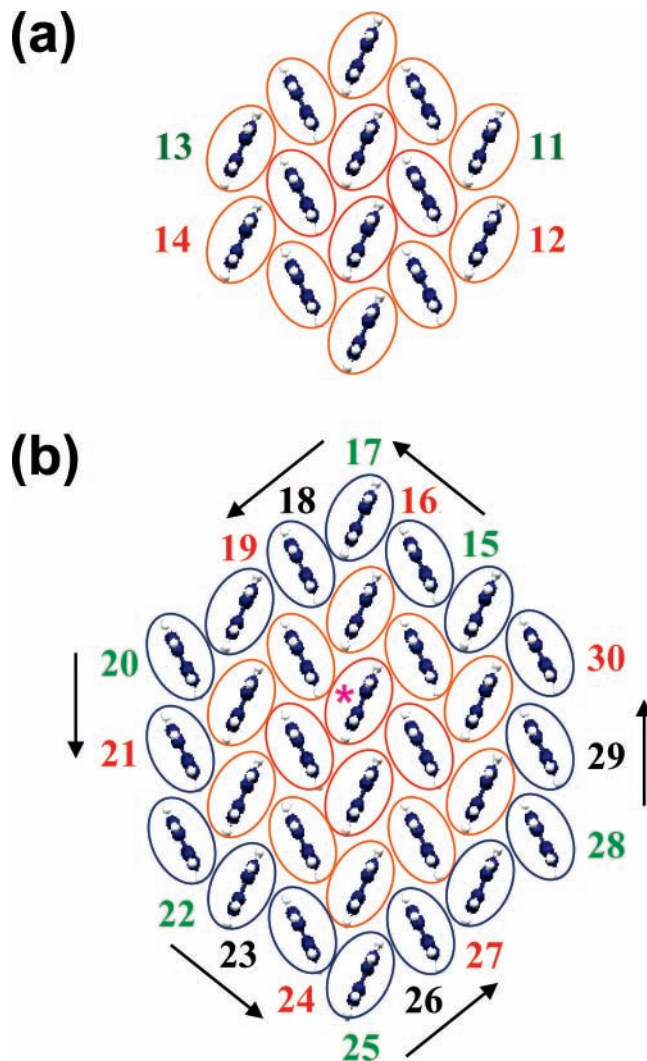

Figure 2. Schematic diagrams for proposed 2D herringbone arrays of (a) the tetracene 14-mer and (b) 30-mer in a perpendicular cross section with respect to the long molecular axes of tetracene. In (a), the stepwise filling of a second 2D shell around a 14-mer is represented by successive additions of molecules numbered from 15 to 30. Red or green numbers correspond to a local maximum or local minimum of the ion distribution of $(tetracene)_n^-$ (see Figure 1b), respectively.

all of these cluster numbers appear as local maxima in the ion distribution of $(tetracene)_n^-$, as seen in Figure 1b. In particular, a highly symmetric shell closure is found at 19, where the one molecule (indicated by an asterisk in Figure 2b) is fully surrounded by 6 first-shell and 12 second-shell molecules. Another type of 2D enclosure at 19 is compatible with the fact that the most prominent maximum appears at $n = 19$ in the mass spectrum. On the other hand, the $n = 15$, 17, 20, 22, 25, and 28 clusters, which appear as local minima in the mass spectrum, possess one constituent molecule that interacts with only two nearest neighbors (i.e., molecule 15, 17, 20, 22, 25, or 28). This is probably the major reason for the less abundant production of these clusters. For $n > 30$, the observed oscillations in mass intensity can be interpreted in terms of subshell closings, but their amplitudes reduce gradually with cluster size. As described below, this decline is due to the population reduction of the 2D clusters (called "isomer II-1" below) at larger sizes.

The even−odd alternation from $n = 10$ to 14 can be also explained by the aforementioned cluster growth model, with the assumption that the $n = 10-14$ clusters correspond to a
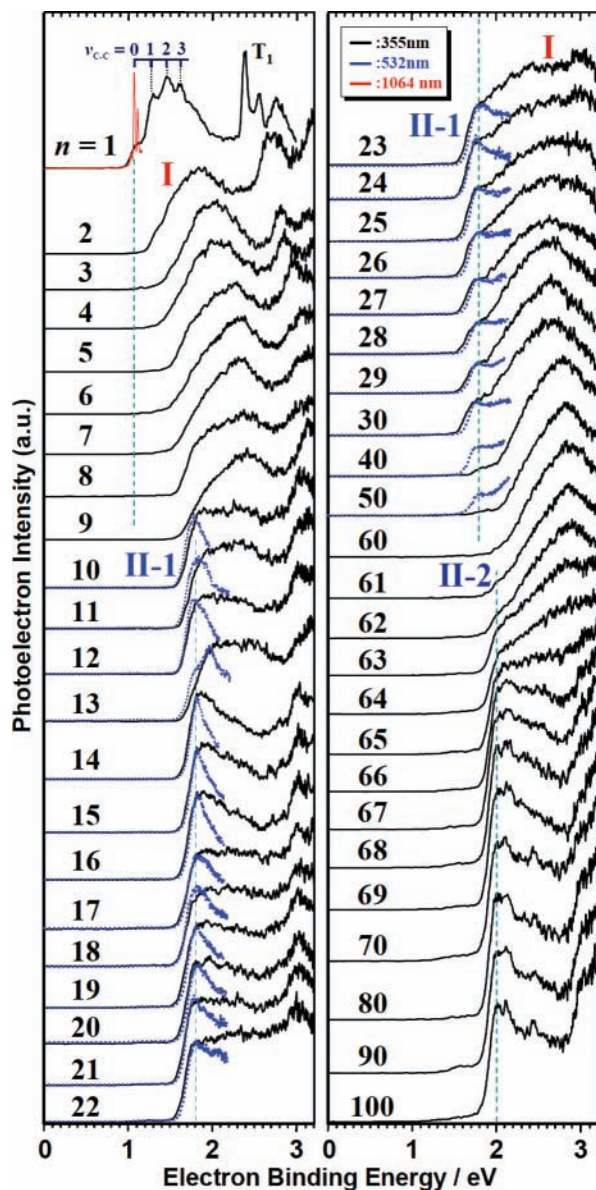
Figure 3. PE spectra for (tetracene)$_n^-$ with $n = 1-100$ measured at 355 nm (3.496 eV), together with the spectra for $n = 1$ taken at 1064 nm (1.165 eV) and the spectra for $n = 10-50$ taken at 532 nm (2.331 eV) with deceleration of the parent ions. Note that the VDEs of band II-1 and band II-2 remain constant at 1.80 and 2.0 eV, respectively.

fragment of the 2D 14-mer unit shown in Figure 2a. For example, the 2D shell around a 10-mer unit can be filled by molecules 11–14, as shown in Figure 2a, and the shell closing is found at 10 and 12, which appear as local maxima in the mass spectrum. For $n < 10$, however, the magic numbers of $n = 5$ and 8 cannot be explained by this model, implying that different types of 2D orderings may occur below $n = 10$. In particularly small sizes, cluster structures (i.e., intermolecular orientations and distances) seem immensely size-dependent; therefore, it is difficult to predict the cluster structures for $n < 10$ at this moment.

Figure 3 shows the PE spectra of (tetracene)$_n^-$ ($n = 1-100$) measured at 355 nm, together with the 1064 nm spectrum of $n = 1$ and the 532 nm spectra of $n = 10-50$. From the 1064 nm spectrum, the adiabatic electron affinity (EA$_a$) of a tetracene molecule is determined to be 1.058 ± 0.005 eV, which agrees well with the literature values.[17] In the 355 nm spectrum for $n = 1$, a bell-shaped envelope having an extensive vibrational progression of the C—C stretching A$_g$ mode of 0.18 eV
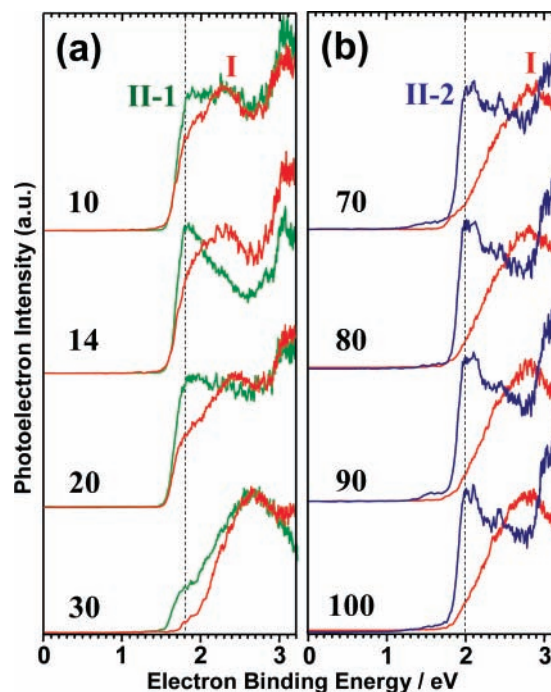

Figure 4. PE spectra for (tetracene)$_n^-$ with (a) $n = 10$, 14, 20, and 30 and (b) 70, 80, 90, and 100, measured under different experimental conditions. In Figure 4(a), the PE spectra (red) and the spectra (green) were measured under the experimental conditions of Figure 1a and b, respectively. In (b), the PE spectra (dark blue) were measured with a helium stagnation pressure of 70 atm, whereas the spectra (red) were measured with a stagnation pressure of 5 atm. The spectral variations show the coexistence of two isomers, (a) isomers I and II-1 or (b) isomers I and II-2.

($\sim$1450 cm^{-1}) is observed,[18] together with the relatively sharp feature representing the photodetachment transition to the lowest excited triplet state (T$_1$) of the neutral around 2.4 eV. From $n = 2$ to 9, the bell-shaped envelope (labeled "I") shifts gradually toward a higher binding energy as the cluster size increases. The unresolved vibrational feature in the spectra of $n \geq 2$ is due to the fact that the number of intermolecular modes excited in the photodetachment process increases rapidly with cluster size.

The spectral features of the $n = 2-9$ clusters (except for $n = 8$) are quite analogous to that of $n = 1$, implying that the excess electron is localized on a single tetracene molecule (i.e., a monomeric anion core) in these clusters. However, the 355 nm PE spectra of $n \geq 10$ exhibit somewhat different spectral envelopes (also somewhat in $n = 8$) from those of $n = 1-7$ and 9, and they appear to contain an additional lower-energy band (labeled "II-1"), together with the higher-energy band I. Particularly, the PE spectra of $n = 14-16$ display an origin-dominant spectral feature of band II-1 in which the (unresolved) vibrational envelope of the C—C stretching A$_g$ mode is much less prominent compared to that seen in band I. As shown in Figure 4a, the PE spectra of $n \geq 10$ vary with the experimental conditions. Band II-1 is observed to be more prominent under the experimental condition of Figure 1b than that of Figure 1a. Hence, it is evident that the two isomers, that is, isomers I and II-1, coexist in the size range of $n = 10-50$, and isomer II-1 corresponds to the two-dimensionally ordered clusters, the presence of which has been revealed by the characteristic ion distribution.

In contrast to isomer I, the vertical detachment energy (VDE) of isomer II-1 does not increase even for an increase in cluster size from $n = 14$ to 50; it stays constant at the value of

Letters

J. Phys. Chem. A, Vol. 111, No. 39, 2007 **9647**

1.80 eV. Interestingly, this signifies that the stepwise stabilization energy added per molecule is almost the same between the anion and the neutral states over the range of $n = 14-50$. Since the ion−neutral electrostatic interactions are much stronger than the neutral−neutral interactions, it can be supposed that there is a significant charge screening effect in isomer II-1. Compatibly, in the 14-mer unit in Figure 2a, 10 tetracene molecules densely fill the first 2D shell around the central tetramer core, thus screening the central excess charge so efficiently. Although it is not clear at present how many central tetracene molecules share the excess electron, the anion core in isomer II-1 might be tetrameric in nature. In such a multimeric anion, the intramolecular nuclear reorganizations of each molecule sharing the excess charge become smaller than that of the monomer anion,[5] resulting in much less prominent excitation of the C−C stretching mode in the photodetachment process than that for the monomer anion. This trend is indeed found in the spectral profile of isomer II-1 (e.g., $n = 14-16$), whose vibrational feature is apparently much less prominent than that of $n = 1$ or isomer I having a monomeric anion core. Importantly, the invariable nature of the VDE also means that degrees of the structural relaxation from the equilibrium geometry of the anion state (i.e., isomer II-1) to that of the neutral state no longer depend on the cluster size over $n = 14$ because the magnitude of the VDE is dominated by not only energetics but also structural factors, that is, intermolecular reorganization. This experimental implication is, in fact, consistent with the establishment of a rigid (or stable) 2D structural unit with a certain ion core at $n = 14$ (see Figure 2a).

As seen in Figure 3, isomer II-1 gradually disappears beyond $n \sim 22$ and barely persists out to $n \sim 50$. Concomitantly, isomer I is the dominant product in the size range of $n = 40-60$ under any source conditions. A further continuous increment in the VDE of isomer I is observed with increasing n due to electronic polarization and intermolecular reorganization of neutral molecules encompassing a monomeric anion core three-dimensionally. As a result, isomer I becomes more energetically stable than isomer II-1 at larger cluster sizes. At this moment, we do not know the structural motifs of isomer I, but the broad PE profiles for this isomer indicate that significant structural reorganizations from their neutral counterparts occur. Furthermore, since the VDE of isomer I persistently increases with n, a charge screening effect may be less efficient in isomer I than that in isomer II-1. Hence, isomer I probably has a less dense packed three-dimensional structure that is far from the 2D dense packing structure seen in isomer-II-1.

Above $n = 60$, a low-energy feature (designated as isomer II-2) appears at a high stagnation pressure of 70 atm and becomes increasingly prominent with increasing cluster size. As shown in Figure 4b, at a low stagnation pressure (5 atm), it is not observed at all, and isomer I is observed exclusively, showing the coexistence of isomers I and II-2. This result indicates that the warmer cluster formation conditions allow for a large rearrangement of cluster geometry upon electron attachment, yielding isomer I, while cold formation conditions prohibit such structural reorganization, leading to isomer II-2. Interestingly, the spectral profile of isomer II-2 is quite similar to those of isomer II-1, and again like isomer II-1, the VDEs of isomer II-2 also do not shift at all up to $n = 150$ (data not shown) and remain constant at 2.0 eV. The close similarity between isomers II-1 and II-2 suggests that they possess kindred structural motifs with a common ion core. One noticeable difference between isomers II-1 and II-2 is that the constant VDE value of isomer II-2 is 0.2 eV larger than that of isomer

II-1 (i.e., 1.80 eV), showing that there are some additional charge stabilization effects in isomer II-2. Since isomer II-2 appears only in much larger sizes ($n > \sim 60$) than a single 2D layer of isomer II-1, we can infer that the isomer II-2 clusters possess a double-layered or more multilayered structural motif, where two or more finite 2D herringbone layers are stacked like those in the tetracene crystal. The additional small stabilization of 0.2 eV may thus arise from polarization of neutral molecules located in adjacent layer(s).

Notwithstanding that isomer II-2 appears on the ~ 0.8 eV lower binding energy side of isomer I, the colder source conditions prefer to produce isomer II-2. This behavior suggests that the rigid, crystal-like anion state (isomer II-2) is energetically (or adiabatically) more stable than the highly reorganized one (isomer I), though the difference between the adiabatic levels of isomers I and II-2 should be very small in energy. It is pertinent to note that the magnitude of the polarization energy is profoundly related to a morphology of molecular aggregation and hence to the molecular packing density of aggregates.[19] In ultraviolet photoelectron spectroscopy of a pentacene solid film, for instance, Sato et al. have reported[20] the increase in the polarization energy for cations (or holes) in going from the amorphous to crystalline state (i.e., 0.3 eV), which is due to an increment of packing density. Hence, the polarization energy of isomer II-2 may be somewhat larger than that of isomer I.

The (vertical) total charge stabilization energies (ΔE_{tot}) for the "crystal-like" isomers II-1 and II-2 are determined to be -0.74 and -0.94 eV, respectively, by summing the EA_a value of a tetracene molecule (ca. 1.06 eV) and each constant $-$VDE value obtained. The former value of -0.74 eV may be viewed as an asymptotic ΔE_{tot} value for a free-standing, infinite 2D tetracene monolayer because of its invariant nature for $n \geq 14$. Interestingly, this value already reaches to about 80% of the effective polarization energies of tetracene crystal (ca. -0.92 eV).[21,22] Moreover, ΔE_{tot} of isomer II-2 (-0.94 eV) is almost entirely in accord with those bulk values. These facts surprisingly demonstrate the largely localized nature of polarization in a cluster analogue of the tetracene single crystal, which has been generally believed to extend over many lattice constants in OMCs.[1]

In summary, we have presented the experimental evidence for the highly localized nature of electronic polarization in $(\text{tetracene})_n^-$. As a key result, we find no VDE shift of the crystal-like clusters (isomers II-1 and II-2), revealing that only 14 tetracene molecules within a 2D herringbone-type layer can provide a charge stabilization energy corresponding to $\sim 80\%$ of that of the crystal, and the rest of the charge stabilization is provided by electronic polarization of neutral molecules in adjacent layers.

References and Notes

(1) Silinsh, E. A.; Capek. V. *Organic Molecular Crystals: Interaction, Localization and Transport Phenomena*; AIP Press: New York, 1994.

(2) Coropceanu, V.; Cornil, J.; da Silva Filho, D. A.; Olivier, Y.; Silbey, R.; Brédas, J. *Chem. Rev.* **2007**, *107*, 926 and references therein.

(3) Pope, M.; Swenberg, C. E. *Electronic Processes in Organic Crystals*; Oxford University Press: London, 1982.

(4) de Boer, R. W. I.; Gershenson, M. E.; Morpurgo, A. F.; Podzorov, V. *Phys. Status Solidi* **2004**, *201*, 1302.

(5) Witte, G.; Wöll, C. *J. Mater. Res.* **2004**, *19*, 1889.

(6) Koch, N.; Vollmer, A.; Salzmann, I.; Nickel, B.; Weiss, H.; Rabe, J. P. *Phys. Rev. Lett.* **2006**, *96*, 156803.

(7) Deng, W. Q.; Goddard, W. A., III. *J. Phys. Chem. B* **2004**, *108*, 8614.

(8) Song, J. K.; Han, S. Y.; Chu, I.; Kim, J. H.; Kim, S. K.; Lyapustina, S. A.; Xu, S.; Nilles, J. M.; Bowen, K. H., Jr. *J. Chem. Phys.* **2002**, *116*, 4477.

(9) Song, J. K.; Lee, N. K.; Kim, S. K. *Angew. Chem.*, *Int. Ed.* **2003**, *42*, 213.

(10) Song, J. K.; Lee, N. K.; Kim, J. H.; Han, S. Y.; Kim, S. K. *J. Chem. Phys.* **2003**, *119*, 3071.

(11) Mitsui, M.; Kokubo, S.; Ando, N.; Matsumoto, Y.; Nakajima, A.; Kaya, K. *J. Chem. Phys.* **2004**, *121*, 7553.

(12) Mitsui, M.; Nakajima, A. *Bull. Chem. Soc. Jpn.* **2007**, *80*, 1058.

(13) Even, U.; Jortner, J.; Noy, D.; Lavie, N.; Cossart-Magos, C. *J. Chem. Phys.* **2000**, *112*, 8068.

(14) Nakajima, A.; Taguwa, T.; Hoshino, K.; Sugioka, T.; Naganuma, T.; Ono, F.; Watanabe, K.; Nakao, K.; Konishi, Y.; Kishi, R.; Kaya, K. *Chem. Phys. Lett.* **1993**, *214*, 22.

(15) Farges, J.; Deferaudy, M. F.; Raoult, B.; Torchet, G. *Surf. Sci.* **1985**, *156*, 370.

(16) Näher, U.; Zimmermann, U.; Martin, T. P. *J. Chem. Phys.* **1993**, *99*, 2256.

(17) Crocker, L.; Wang, T.; Kebarle, P. *J. Am. Chem. Soc.* **1993**, *115*, 7818 and references therein.

(18) Kato, T.; Yamabe, T. *J. Chem. Phys.* **2001**, *115*, 8592.

(19) Sato, N.; Seki, K.; Inokuchi, H. *J. Chem. Soc.*, *Faraday Trans. 2* **1981**, *77*, 1621.

(20) Sato, N.; Seki, K.; Inokuchi, H.; Harada, Y. *Chem. Phys.* **1986**, *109*, 157.

(21) Sato, N.; Inokuchi, H.; Silinsh, E. A. *Chem. Phys.* **1987**, *115*, 269.

(22) Eisenstein, I.; Munn, R. W. *Chem. Phys.* **1983**, *77*, 47.